Working Paper

On the Role of Body Size in a Tri-Trophic Metapopulation Model

S. Rinaldi
S. Dal Bo
E. De Nittis

WP-95-72
July 1995

IIASA International Institute for Applied Systems Analysis □ A-2361 Laxenburg □ Austria
Telephone: +43 2236 807 □ Fax: +43 2236 71313 □ E-Mail: info@iiasa.ac.at

On the Role of Body Size in a Tri-Trophic Metapopulation Model

S. Rinaldi
S. Dal Bo
E. De Nittis

WP-95-72
July 1995

International Institute for Applied Systems Analysis □ A-2361 Laxenburg □ Austria
Telephone: +43 2236 807 □ Fax: +43 2236 71313 □ E-Mail: info@iiasa.ac.at

ON THE ROLE OF BODY SIZE IN A TRI-TROPHIC METAPOPULATION MODEL*

S. Rinaldi[a], *S. Dal Bo*[b], *E. De Nittis*[b]

*This work has been partially supported by the International Institute for Applied Systems Analysis (IIASA), Laxenburg, Austria, and by the Italian Ministry of Scientific Research and Technology, contract MURST 40% Teoria dei sistemi e del controllo.

[a]Centro Teoria dei Sistemi, CNR, Politecnico di Milano, Milano, Italy.

[b]Master student at the Politecnico di Milano, Milano, Italy.

Abstract

A particular tri-trophic (resource, prey, predator) metapopulation model with dispersal of preys and predators is considered in this paper. The analysis is carried out numerically, by finding the bifurcations of the equilibria and of the limit cycles with respect to prey and predator body sizes. Two routes to chaos are identified. One is characterized by an intriguing cascade of flip and tangent bifurcations of limit cycles, while the other corresponds to the crisis of a strange attractor. The results are summarized by partitioning the space of body sizes in eight subregions, each one of which is associated to a different asymptotic behavior of the system. Emphasis is put on the possibility of having different modes of coexistence (stationary, cyclic, and chaotic) and/or extinction of the predator population.

1. Introduction

A particular tri-trophic (resource, prey, predator) metapopulation model composed by five ODEs is discussed in this paper. The first three equations describe the dynamics of the resource patches which are, respectively, free, colonized by preys, or by preys and predators. The two remaining equations on the contrary, describe the dynamics of the densities of prey and predator dispersed in the environment. Models of this kind have been first proposed by Levins (1969, 1970) to analyze the role played by spatial inhomogeneity of populations without making use of partial differential equations. The reader interested in more details can refer to Diekmann *et al.* (1988) for the derivation and interpretation of such kind of models and to Taylor (1990) for a critical review on the role of dispersal.

The model studied in this paper is a natural extension of those discussed in Sabelis *et al.* (1991), Jansen and Sabelis (1992), and Jansen (1995). The aim is to establish the role played by prey and predator body sizes in determining the asymptotic behavior of the system. Bifurcation curves are produced numerically in the two-dimensional parameter space of body sizes, in order to identify the regions where stationary, cyclic, or chaotic coexistence is possible. Hopf bifurcations of equilibria, as well as tangent, flip, and transcritical bifurcations of limit cycles and catastrophic bifurcations of strange attractors (Arnold, 1983; Guckenheimer and Holmes, 1983) are detected. They prove that alternative regimes of coexistence are possible for suitable combinations of the body sizes, while for other combinations the extinction of the predator is guaranteed. Actually, such a region of extinction is surrounded by a region of chaotic coexistence. By varying the body sizes one can enter the region of chaotic regime in two distinct ways: through an infinite cascade of local bifurcations or suddenly, i.e., without any warning in terms of bifurcations. Nevertheless, it is interesting to note that these two routes to chaos are only two different aspects of the same bifurcation structure (a complex cascade of intersecting flip and tangent bifurcation curves).

The paper is organized as follows. In the next section the model is briefly described, while in Sections 3 and 4 its equilibrium and limit cycles are discussed in some detail with emphasis on their bifurcations. Then, in Section 5, the two possible routes to chaos are pointed out and the region of extinction of the predator population is identified.

A summary and some interpretations of the results conclude the paper.

2. The Model

The tri-trophic metapopulation model we analyze in this paper is composed of patches of resource, preys, and predators. With the capital letters X, Y, and Z we indicate, in suitable units,

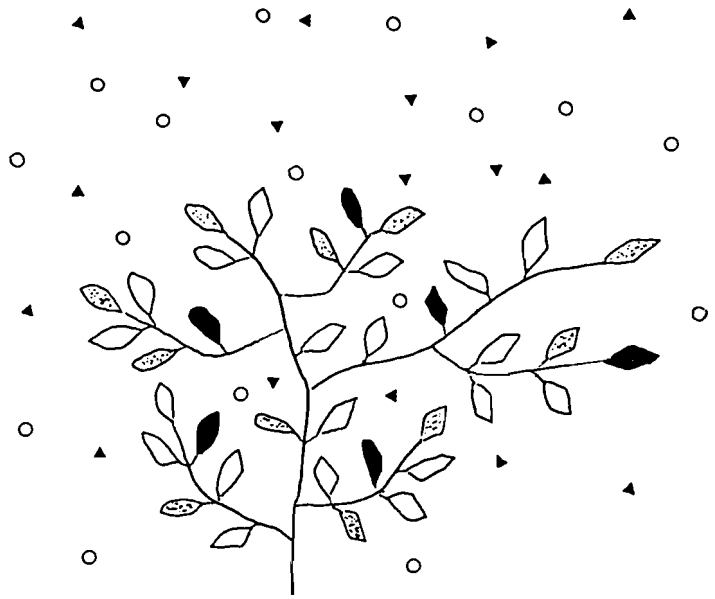

Figure 1. A symbolic sketch of the system: white, gray, and black leaves are free (X), prey (Y), and predator (Z) patches; empty circles and black triangles are prey (y) and predator (z) dispersers.

the number of free patches, the number of patches occupied only be preys (called prey patches) and the number of patches occupied by preys and predators (called predator patches). Typical examples of such systems are populations of parasites and insects living patchly on plants. Figure 1 shows a symbolic sketch of the system where free, prey, and predator patches are white, gray, and black leaves, while prey dispersers and predator dispersers (indicated in the following with the lower case letters y and z) are represented by empty circles and black triangles.

The dynamic behavior of the system is described by the following five differential equations:

$$\dot{X}(t) = rX(t)\left(1 - \frac{X(t)}{K}\right) - a_1 \frac{X(t)}{b_1 + X(t)} y(t) \tag{1}$$

$$\dot{Y}(t) = a_1 \frac{X(t)}{b_1 + X(t)} y(t) - d_1 Y(t) - a_2 \frac{Y(t)}{b_2 + Y(t)} z(t) \tag{2}$$

$$\dot{Z}(t) = a_2 \frac{Y(t)}{b_2 + Y(t)} z(t) - d_2 Z(t) \tag{3}$$

$$\dot{y}(t) = \frac{1}{\sigma_y}\left(d_1 Y(t) - m_1 y(t)\right) \tag{4}$$

$$\dot{z}(t) = \frac{1}{\sigma_z}\left(d_2 Z(t) - m_2 z(t)\right) \tag{5}$$

where the 12 parameters, $\sigma_y, \sigma_z, r, K, a_i, b_i, d_i, m_i, i = 1, 2$, are assumed to be constant (i.e., seasonalities are not taken into account).

The first term on the right-hand side of equation (1) says that in the absence of prey dispersers ($y = 0$) the free patches grow logistically (r is the net growth rate per capita, and K is the carrying capacity), while the second term is the rate at which free patches are invaded and transformed into prey patches [see first term of equation (2)]. The rate of invasion is proportional to the abundance of prey dispersers and to the probability that a disperser comes across a free patch. Such a probability, obviously, increases from zero to one with the density of free patches.

Many functional forms could be given to this probability, but the one which has been chosen here, namely the Monod form $X/(b_1 + X)$, is particularly convenient, as shown below, because it allows one to link model (1-5) with the most classical food chain model (characterized by Holling type-II functional responses). Similar considerations hold for the rate at which prey patches are invaded by predator dispersers z and thus transformed into predator patches [see third term of equation (2) and first term of equation (3)]. The second terms of equations (2) and (3) are the death rates of occupied patches: they simply say that, in the absence of dispersion, occupied patches would be consumed exponentially with average life time equal to $1/d_i$. Since the time needed by a colony of prey to consume the resource of a patch is smaller when such a colony is not controlled by its predator, we will consider, in the following, systems with $d_1 > d_2$. Finally, equation (4) [equation (5)] describes the dynamics of prey [predator] dispersers: it is the balance between the inflow rate due to the release of preys [predators] into the environment from a consumed prey [predator] patch and the mortality rate due to starvation (predation is possible only on patches).

Model (1-5) differs from the models discussed in Sabelis *et al.* (1991), Jansen and Sabelis (1992), and Jansen (1995) for two reasons: first, because both species are dispersed at the same time and second, and most important, because the rates of invasion of free an prey patches do not increase indefinitely with the number of such patches. On the contrary, the models discussed in the above-mentioned papers are characterized by rates of invasion proportional to the number of invadable patches. This means that in these models the term $a_1X/(b_1 + X)$ in equation (1) is substituted by its linear approximation at low values of X, namely a_1X/b_1. This is somehow justified if the carrying capacity of the resource is small compared to b_1, i.e., if $K << b_1$, because the inequality $X(t) \leq K$ implies $X(t) << b_1$. But in the opposite case, the saturation of the invasion rate with respect to X plays an important role. In order to stress this role, we will consider metapopulations with $K > b_1$.

In the following, all possible asymptotic modes of behavior of system (1-5) will be classified for all positive values of the parameters $\sigma_y$and σ_z, keeping all other parameters fixed at a reference value specified below. It is therefore convenient to give a simple biological interpretation of σ_y and σ_z. For this, assume that each time the resource of a prey patch is exhausted, there is a release in the environment of N_y preys and that this number is negatively correlated with the body size s_y of the prey, i.e., $N_y \equiv 1/s_y$. But it is also fair to assume that the mortality of a prey disperser is inversely proportional to its body size, i.e., $M_y \equiv 1/s_y$, so that

$$\dot{y}(t) = d_1Y(t)N_y - M_y y(t) = N_y \left(d_1Y(t) - \frac{M_y}{N_y} y(t)\right)$$

By introducing the new parameters σ_y and m_1, this equation can be written in the form (4)

$$\dot{y}(t) = \frac{1}{\sigma_y} \left(d_1Y(t) - m_1 y(t)\right)$$

with σ_y proportional to body size and m_1 independent upon body size. The same argument applies to predator dispersers, and the conclusion is that the two parameters σ_y and σ_z can be considered to be a measure of the body sizes of the individuals of the two species. Very small values of such parameters correspond to the case of very small parasites and insects which are very quickly dispersed into the environment. In the limit case ($\sigma_y \to 0, \sigma_z \to 0$) (instantaneous dispersion) we can use the singular perturbation argument to conclude that

$$y(t) = \frac{d_1}{m_1} Y(t) \qquad z(t) = \frac{d_2}{m_2} Z(t)$$

i.e., densities of preys and predators dispersed in the environment are proportional to the abundance of prey and predator patches. Substituting these relationships into equations (1-3) we obtain the *reduced metapopulation model*

$$\dot{X}(t) = \left[r\left(1 - \frac{X(t)}{K}\right) - c_1 \frac{Y(t)}{b_1 + X(t)} \right] X(t) \tag{6}$$

$$\dot{Y}(t) = \left[c_1 \frac{X(t)}{b_1 + X(t)} - d_1 - c_2 \frac{Z(t)}{b_2 + Y(t)} \right] Y(t) \tag{7}$$

$$\dot{Z}(t) = \left[c_2 \frac{Y(t)}{b_2 + Y(t)} - d_2 \right] Z(t) \tag{8}$$

where $c_i = a_i d_i / m_i, i = 1, 2$. Such a model is the classical Rosenzweig-McArthur food chain model which has been extensively studied during the last few years through singular perturbation analysis (Muratori, 1991; Muratori and Rinaldi, 1991, 1992; Rinaldi and Muratori, 1992; Kuznetsov *et al.*, 1995) simulation (Hastings and Powell, 1991; Scheffer, 1991; Abrams and Roth, 1994a, 1994b; McCann and Yodsiz, 1994) and bifurcation analysis (Klebanoff and Hastings, 1994; McCann and Yodsiz, 1995a; Kuznetsov and Rinaldi, 1995). It has a very rich bifurcation structure showing that stable coexistence of the three species can be stationary, cyclic, or chaotic. There are multiple attractors and in some cases there are even alternative stable regimes of coexistence. In many regions of the parameter space a degenerate attractor corresponding to the extinction of the top predator (Z) is present together with a strictly positive attractor (coexistence), thus meaning that the long-term survival of the top predator population can be critically related to the timing and amplitude of the disturbances acting on the system.

Since model (1-5) is an extension of model (6-8), one should expect for model (1-5) a bifurcation structure at least as complex as that pointed out in Klebanoff and Hastings (1994), McCann and Yodsiz (1995a), Kuznetsov and Rinaldi (1995). Here, in order to avoid paramount analyses of the bifurcations of model (1-5), only the parameters σ_y and σ_z [which do not appear in model (6-8)] will be varied. For this reason, the remaining parameters of model (1-5) have been fixed to the following reference values

$$r = 1 \quad K = 1$$

$$a_1 = \frac{5}{3} \quad b_1 = \frac{1}{3} \quad d_1 = \frac{2}{5} \quad m_1 = \frac{2}{5}$$

$$a_2 = \frac{5}{100} \quad b_2 = \frac{1}{2} \quad d_2 = \frac{1}{100} \quad m_2 = \frac{1}{100}$$

which satisfy the conditions $K > b_1$ and $d_1 > d_2$ pointed out earlier. For these values of the

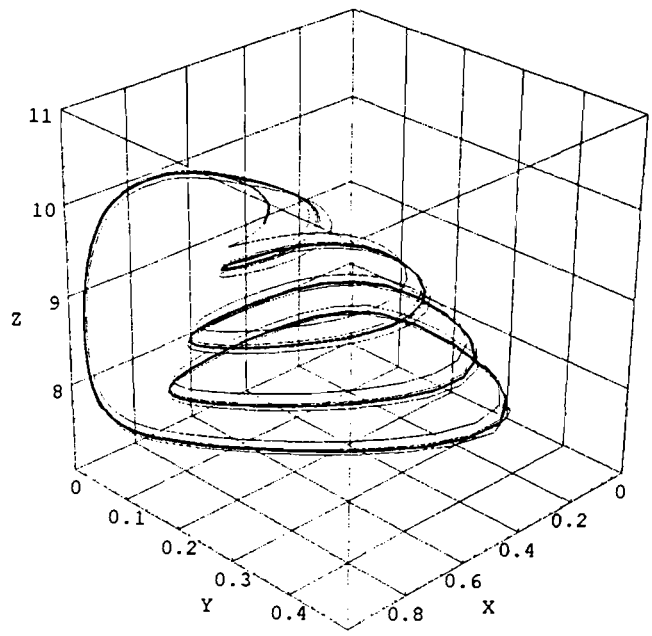

Figure 2. A three-dimensional view of the "tea-cup" strange attractor A of the reduced model (6-8).

parameters the reduced model (6-8) has a unique attractor which is a strange attractor indicated by A and known as a *tea-cup* strange attractor (Hasting and Powell, 1991); see Figure 2. This means that the metapopulation model (1-5) with very small values of σ_y and σ_z, i.e., with almost instantaneous dispersion, has only one asymptotic mode of behavior, corresponding to chaotic coexistence. The analysis will point out the effects of body size on this mode of behavior and therefore show how dispersion can stabilize chaos. It is important to stress, however, that the conclusions are valid for the particular parameter setting which has been selected. It might easily be that for other parameter settings, interpreting, for example, specific biological communities, the effects of dispersion would be different.

3. Equilibria

In this section the equilibria of system (1-5) (which do not depend upon σ_y and σ_z) are analyzed and their stability is discussed with respect to σ_y and σ_z. The analysis is quite standard and based mainly on the Jacobian of system (1-5). For this reason the main properties are stated without proof.

There are at most six constant solutions of system (1-5) but one of them is biologically not meaningful because some of the state variables are negative for all combinations of the parameters. Three of the remaining equilibria, namely

$E_0 = (0, 0, 0, 0, 0)$

$E_1 = (K, 0, 0, 0, 0)$

$E_2 = \left(\frac{b_1 m_1}{a_1 - m_1}, \frac{b_1 m_1 r(a_1 K - m_1 K - b_1 m_1)}{d_1 K (a_1 - m_1)^2}, 0, \frac{b_1 (a_1 K - m_1 K - b_1 m_1)}{K (a_1 - m_1)^2}, 0\right)$

are trivial equilibria characterized by the absence of the predator ($Z = z = 0$). For the reference parameter setting, E_2 is positive and all three equilibria are saddles (E_0 and E_1 have only one positive eigenvalue, while E_2 has three positive eigenvalues). Moreover, it can be shown, by analyzing the Jacobian of the system restricted to equations (1, 2, 4) with $Z = z = 0$, that the equilibria E_0, E_1, and E_2 are saddles also in $R^3 = (X, Y, y)$. This implies that if free patches are at their carrying capacity K and there are no preys and predators, after a generic injection of preys the system will tend toward a cycle or a strange attractor in $R^3 = (X, Y, y)$ because the solutions of (1-5) are, in any case, bounded.

The two remaining equilibria, if they exist, are non-trivial and differ only in the first component (X). Both of them can be strictly positive, but for the reference parameter setting only one of them, namely

$E = \left(\frac{4+\sqrt{34}}{12}, \frac{1}{8}, \frac{50\sqrt{34}-115}{18}, \frac{1}{8}, \frac{50\sqrt{34}-115}{18}\right)$

is such. The determinant of the Jacobian evaluated at point E is equal to $-1.73 \cdot 10^{-5}/\sigma_y \sigma_z$ (easy to check) and is therefore negative for all values of σ_y and σ_z. This implies that E cannot undergo saddle-node, pitchfork, and transcritical bifurcations, while Hopf bifurcations are not excluded. Indeed, by applying the Hurwitz criterion to the coefficients of the characteristic polynomial of the Jacobian one can determine the Hopf bifurcation curve shown in Figure 3. Further analysis is needed to establish if this Hopf bifurcation is subcritical or supercritical (as expected for biological reasons). This has been done by means of LOCBIF, a specialized software for the analysis of local bifurcations (Khibnik *et al.*, 1993) and the result is that the Hopf bifurcation is indeed supercritical. Thus, in the vicinity of curve H and below it, the equilibrium E is asymptotically stable, while above that curve the equilibrium is a saddle and there exists a strictly positive stable cycle C in R^5.

4. Cycles

In the previous section it has been shown that above curve H of Figure 3 there exists a stable limit cycle C which is strictly positive (cyclic coexistence). Examples of this cycle are shown in Figure 4 for increasing values of predator body size (σ_z). The geometry of these cycles is rather similar to that of the strange attractor A of the reduced model (see Figure 2). This is an obvious sign (but not a proof) that A is obtained from C through a series of bifurcations. Such bifurcations are described in the next section because they represent one of the two routes to chaos of system (1-5).

Let us then describe the cycles of system (1-5) which cannot be obtained from C through

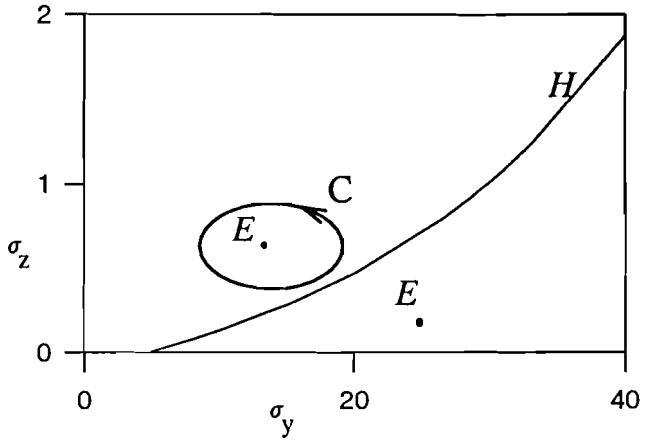

Figure 3. The Hopf bifurcation curve H of the positive equilibrium E. Below the curve E is stable, while above it is unstable (saddle). The closed orbit is a symbolic representation of the positive stable cycle C.

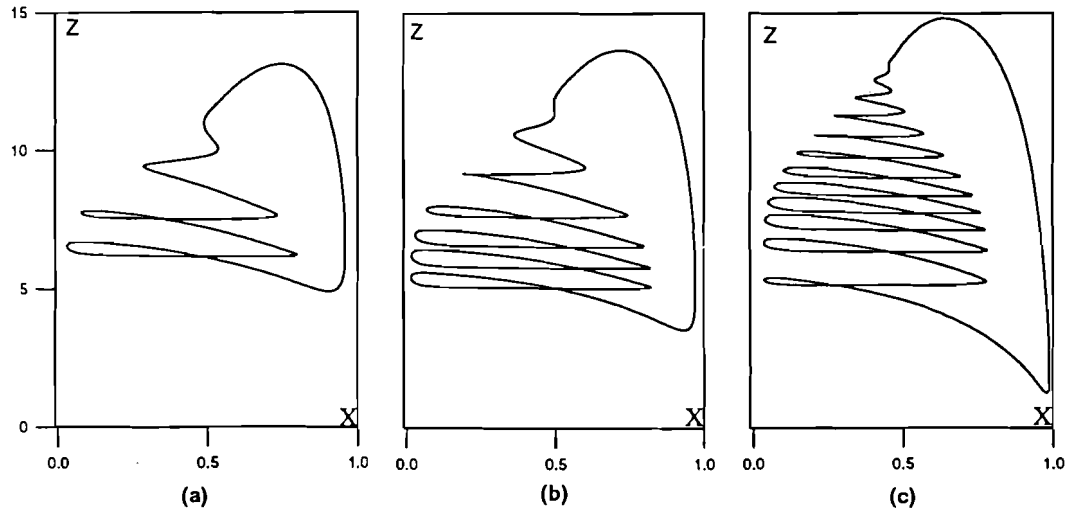

Figure 4. Two-dimensional projection of the positive stable cycle C for $\sigma_y = 5$ and (a) $\sigma_z = 0.5$, (b) $\sigma_z = 1$, (c) $\sigma_z = 5$. For increasing values of predator body size the cycle becomes a "tea-cup" cycle (compare with Figure 2).

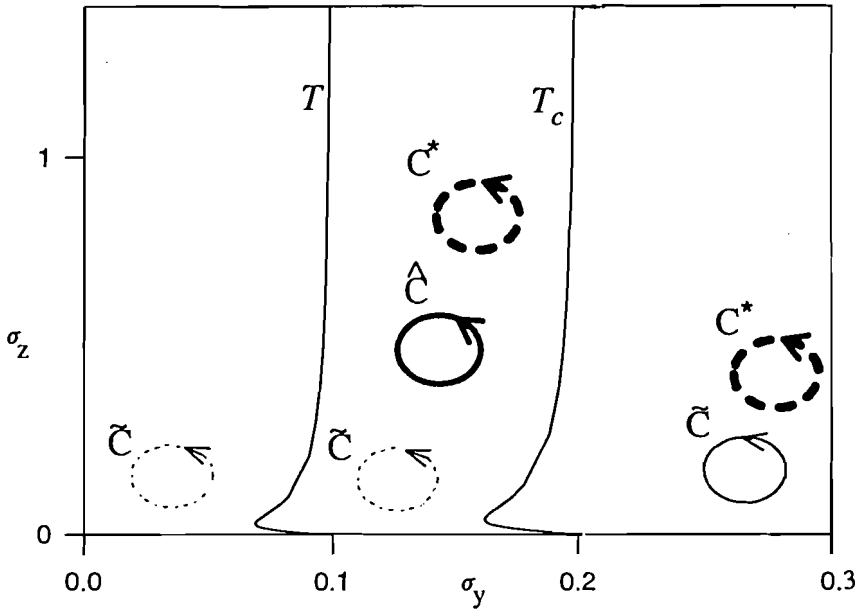

Figure 5. Tangent (T) and transcritical (T_c) bifurcations of cycles. The heavy cycles C^* and $\hat{C}$ are positive cycles (corresponding to cyclic coexistence of all species). The light cycle $\tilde{C}$ is a degenerate cycle characterized by predator extinction ($Z = z = 0$). The dashed cycles are saddle cycles, while the others are stable.

bifurcation. For this, let us make reference to Figure 5 where these cycles are symbolically shown in three different regions of the parameter space. Some of them (heavy lines) are strictly positive cycles (coexistence), while the others (light lines) are in R^3_+ (predator extinction). Moreover, the dashed cycles are saddles (in R^5) while the others are stable (there are no repelling cycles). The two curves indicated by T and T_c are, respectively, tangent and transcritical bifurcations of cycles. They have been obtained by "continuation" using a version of LOCBIF oriented to local bifurcations of limit cycles. In the left region of Figure 5 there is only one cycle denoted by $\tilde{C}$, which is stable in $R^3 = (X, Y, y)$ but unstable in R^5. There are no other attractors in R^3_+ (recall that the three equilibria E_0, E_1, E_2 are saddles). The cycle $\tilde{C}$ becomes stable when the transcritical curve T_c is crossed from the left. Indeed, approaching this curve, a stable and strictly positive cycle $\hat{C}$ gets closer and closer to $\tilde{C}$ and finally collides with it on T_C and leaves the positive octant R^5_+. On the left boundary of the central region (tangent bifurcation curve T) the cycle $\hat{C}$ disappears by colliding with a strictly positive saddle cycle C^*. This saddle cycle C^* is always present on the right side of curve T and is responsible of the "crisis" of strange attractors, as pointed out in the next section.

Although the cycle $\hat{C}$ indicates a possible stable mode of cyclic coexistence, it plays a minor role in the dynamic behavior of system (1-5), because the central region of Figure 5 is rather narrow (compare with Figure 3). Of course, it might be that for different parameter settings this region is larger. In any case, the cycle $\hat{C}$ is quite close to the cycle $\tilde{C}$, with which it collides

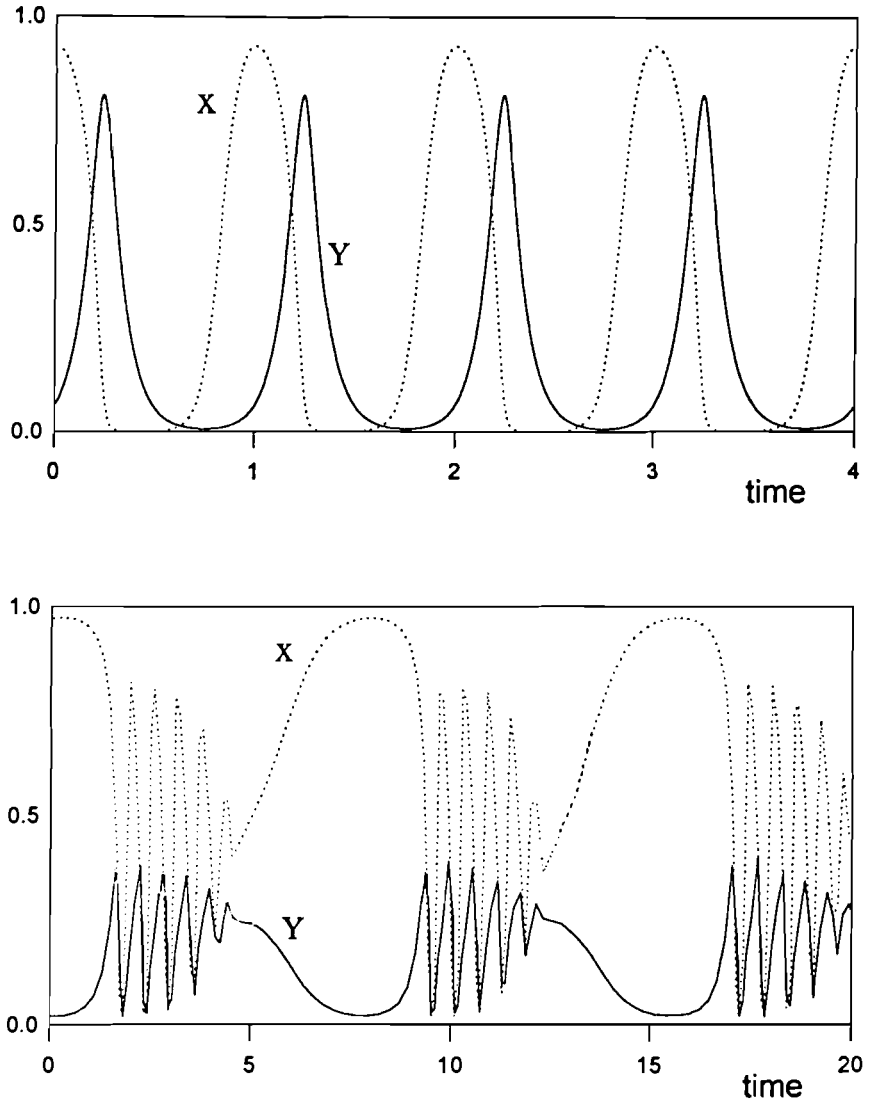

Figure 6. Time series of free patches (X) and prey patches (Y) associated to the two possible modes of cyclic coexistence: (a) the cycle $\hat{C}$ for $\sigma_y = 0.12, \sigma_z = 0.1$; (b) the cycle C for $\sigma_y = 5, \sigma_z = 1$.

on T_c. This means that the coexistence corresponding to $\hat{C}$ is characterized by low numbers of predators so that the oscillations of prey patches are much more relevant than for the cycle C discussed at the beginning of this section. Figure 6 reports the oscillations of free and prey patches in the two possible modes of cyclic coexistence. Notice that the cycle C is characterized by lower peaks of prey patches and by relatively long periods of time during which free patches are almost at their carrying capacity and prey patches are almost absent. This is obviously a more desirable behavior if the prey is actually a pest.

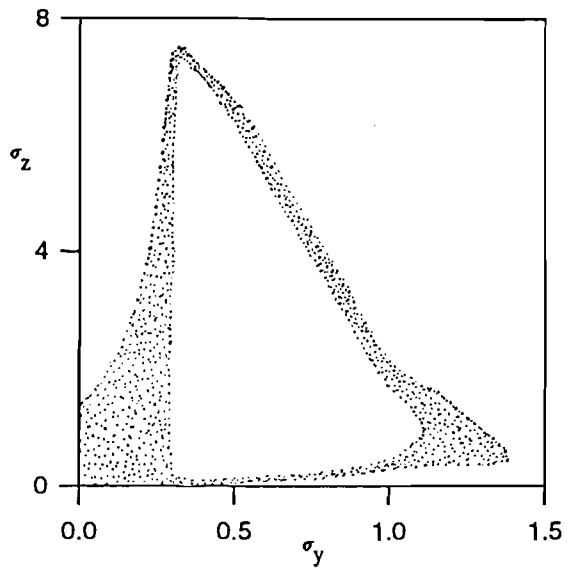

Figure 7. The annular chaotic region (in gray). In the internal white closed region the predator population is doomed to extinction.

5. Routes to Chaos and Strange Attractors

As already said, the reduced-order system (6-8) has a unique strictly positive attractor which is the tea-cup strange attractor shown in Figure 2. By continuity, one can therefore expect that system (1-5) has also a strange attractor for small values of σ_y and σ_z. Indeed, the analysis confirms this fact and shows that strange attractors are confined into the annular region shown in Figure 7. In the closed region delimited by the internal boundary of the chaotic region there is only one attractor, namely the stable cycle $\tilde{C}$ (compare with Figure 5). This means that in this region the extinction of the predator is guaranteed, while in the surrounding region all species can coexist in a chaotic regime. Figure 7 shows that there are two distinct routes to chaos: one through the external boundary and one through the internal boundary of the annular region.

The first route to chaos, namely the one through the external boundary, has to do with a rather complex cascade of flip and tangent bifurcations of the stable limit cycle C. Figure 8 shows the first flip (F) and tangent (T) bifurcation curves of this cascade in a region corresponding to a very thin horizontal band of Figure 7. The flip curves are intersecting one another and a horn delimited by two tangent bifurcation curves emerges between any pair of flip curves. Let us isolate one of these flip curves and the two adjacent tangent horns, as done in Figure 9a and let us decrease σ_y keeping σ_z constant along line (a). Approaching from the right the lowest tangent horn, the cycle C smoothly varies its shape and its period τ, as indicated in Figure 9b. For parameter values inside the horn there exist three limit cycles: two are stable (C and C_2) and one is a saddle (C_1^s). Leaving this horn through the branch T_1, the cycles C and C_1^s collide and disappear, so that only one attractor remains, namely C_2. Decreasing σ_y further,

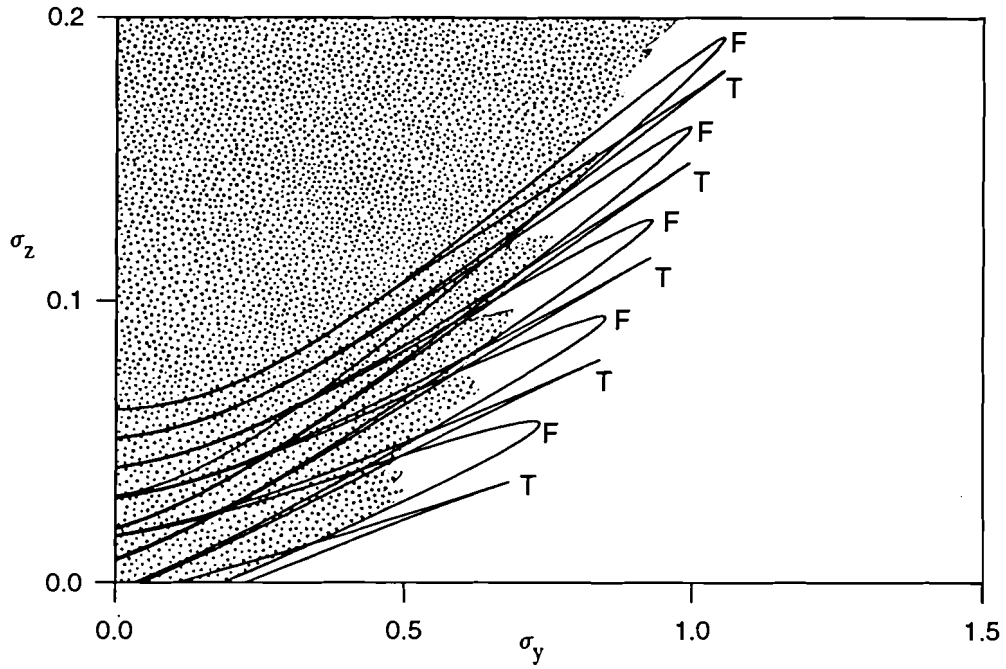

Figure 8. The first flip (F) and tangent (T) bifurcation curves of the positive cycle C and the chaotic region (in gray). Notice the difference in scale with respect to Figure 7.

the cycle C_2 undergoes a flip bifurcation on F_1 giving rise to a stable cycle of double period C_2^2 (not indicated in Figure 9b) and to a saddle cycle C_2^s, which, in turn, undergoes a reverse flip bifurcation on the flip curve F_2. At this point, C_2^s is transformed into a stable cycle C_3, which later disappears by colliding with the saddle cycle C_3^s on T_3. The cycle C_3^s collides also with a stable cycle C_4 on the right branch T_4 of the highest horn. And the story continues like this indefinitely through an alternation of flip and tangent bifurcations. The analysis shows that the stable cycle C originates a sequence of stable cycles $C_2, C_3, C_4, \ldots$. Moreover, every even element of this sequence, namely $C_2, C_4, \ldots$, undergoes a flip bifurcation giving rise to a stable cycle of double period $C_2^2, C_4^2, \ldots$. But the story is endless, because each one of these cycles is the origin of a new cascade of flip and tangent bifurcations. Figure 10 shows, for example, the first flip and tangent bifurcation curves of the cycle C_2^2. Going into the limit, the tangent horns become infinitely many and infinitely thin and form the external boundary of the chaotic region. In practice, the process of accumulation of the flip and tangent curves is very strong and the boundary of the chaotic region can be fairly well approximated by stopping the computations at the third flip (as done for producing Figure 7). In conclusion, approaching the annular chaotic region from outside, one goes through a cascade of catastrophic transitions associated to the tangent horns alternated with non-catastrophic period doublings. This route to chaos is very similar to that discussed in detail in Kuznetsov and Rinaldi (1995) for the reduced-order system (6-8).

The second route to chaos, namely that through the internal boundary of the annular chaotic

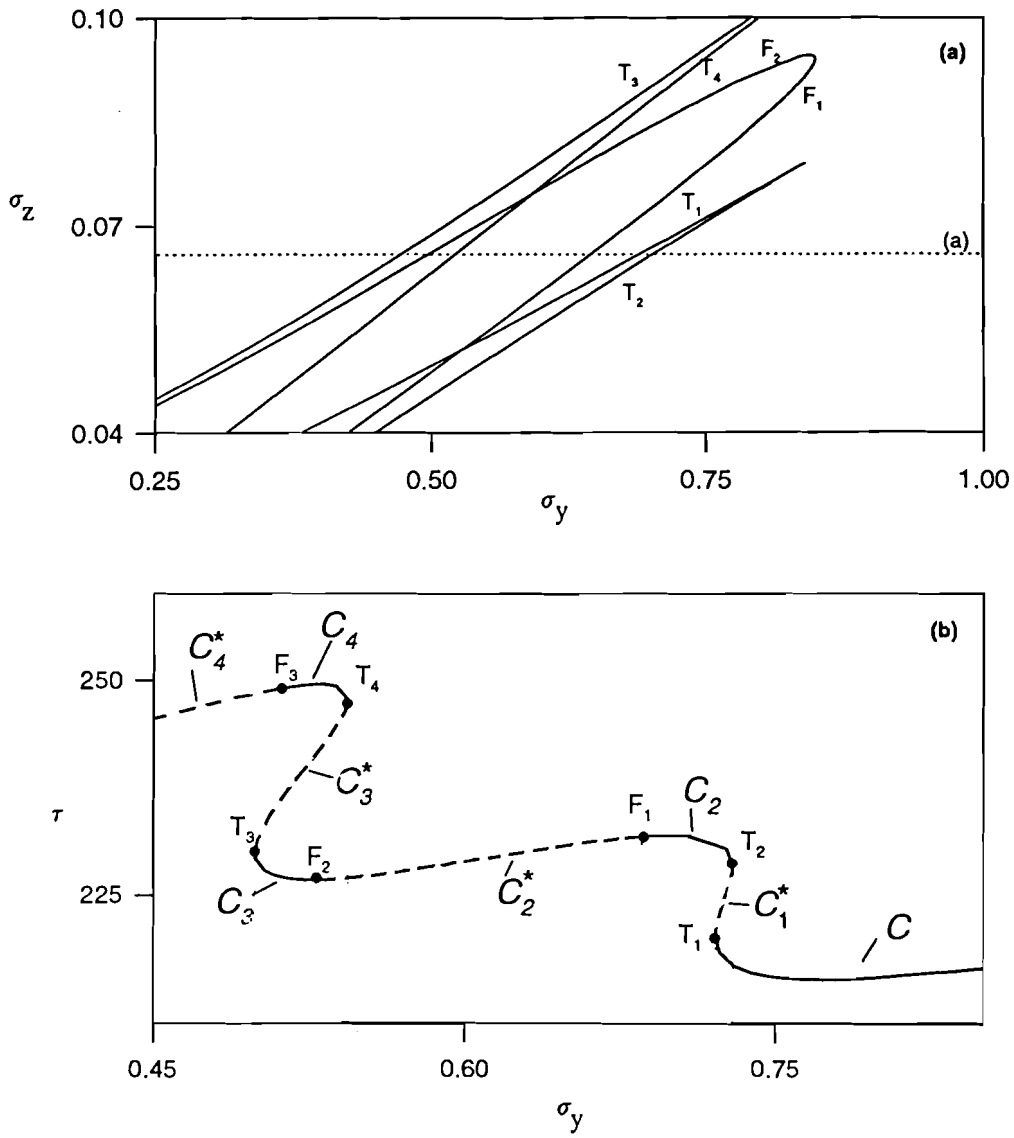

Figure 9. (a) a flip bifurcation curve (F_1, F_2) and the two associated tangent horns (T_1, T_2) and (T_3, T_4); (b) the period τ of the stable (continuous line) and saddle (dashed line) limit cycles obtained from C when moving along the straight line (a) of Figure 9a.

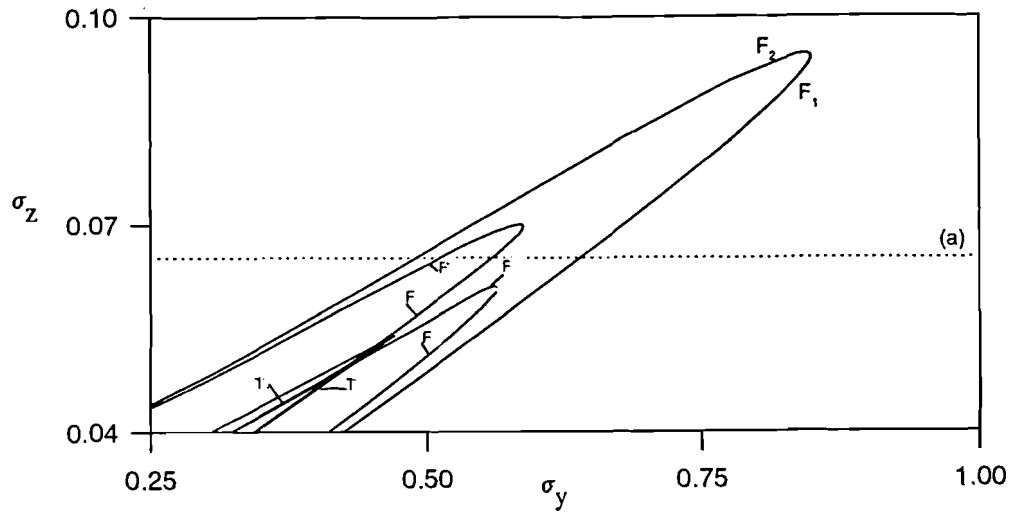

Figure 10. The first flip (F) and tangent (T) bifurcation curves of the cycle C_2^2.

region of Figure 7, is not preceded by any local bifurcation. In other words, the strange attractor appears suddenly without any warning as first noticed by McCann and Yodsiz (1995b) for the reduced model (6-8). Indeed, the internal boundary of the chaotic region is a catastrophic bifurcation corresponding to the collision of the strange attractor with a saddle cycle [a so-called "crisis" (Grebogi, 1983)]. This can be seen by following the strange attractor A and the saddle cycle C^* for different values of σ_y keeping σ_z constant. Figure 11 is a neat example of this sort of numerical experiment: the saddle cycle approaches the strange attractor if σ_y is decreased from 1.07 to 0.83 and soon after that, for $\sigma_y = 0.79$, the collision takes place and the strange attractor disappears. The internal boundary of the chaotic region can be systematically determined by fixing σ_z and producing a bifurcation diagram with respect to σ_y like that shown in Figure 12, where $Z_{\max}$ is the value of Z on the Poincaré section $\dot{Z} = 0$. The points $\underline{\sigma}_y$ and $\overline{\sigma}_y$ at which this bifurcation diagram is interrupted are the coordinates at which the saddle cycle C^* collides with the strange attractor. Figure 7 has been produced in this way by systematically varying σ_z over the whole range of interest.

Finally it is worthwhile noticing that the flip and tangent bifurcation curves forming the cascades described above, start outside the chaotic region (as shown in Figure 8) but tend toward the internal boundary of such a region by spiraling around it. Figure 13 shows one example of these spirals. The figure is only a qualitative sketch, because it was impossible to continue the flip bifurcation curves when approaching the internal boundary of the chaotic region. Nevertheless, the fragments of the curves that have been produced strongly support the conjecture that the two routes to chaos are different aspects of the same bifurcation structure.

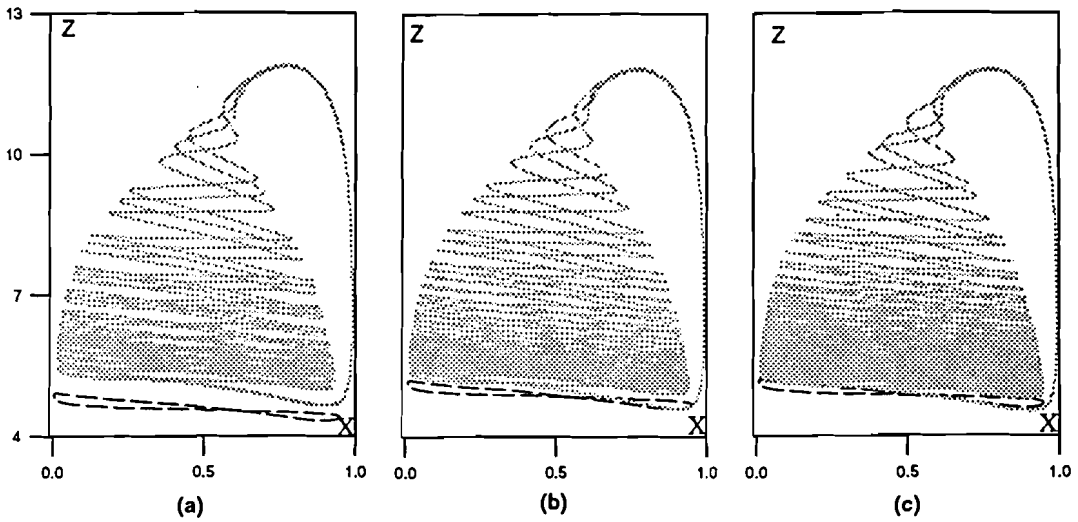

Figure 11. The crisis of the strange attractor. For decreasing values of σ_y the saddle cycle C^* approaches the "tea-cup" strange attractor A. Parameter values are $\sigma_z = 0.3$, (a) $\sigma_y = 1.07$, (b) $\sigma_y = 0.95$, (c) $\sigma_y = 0.83$.

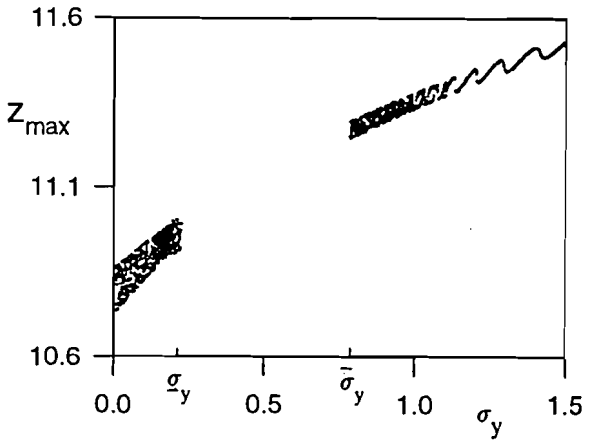

Figure 12. Bifurcation diagram for $\sigma_z = 0.3$ showing the crisis of the strange attractor at $\sigma_y = \underline{\sigma}_y$ and $\sigma_y = \bar{\sigma}_y$. On the vertical axis $Z_{\max}$ represents the value of the variable Z on the Poincaré section defined by $\dot{Z} = 0$ [see equation (3)].

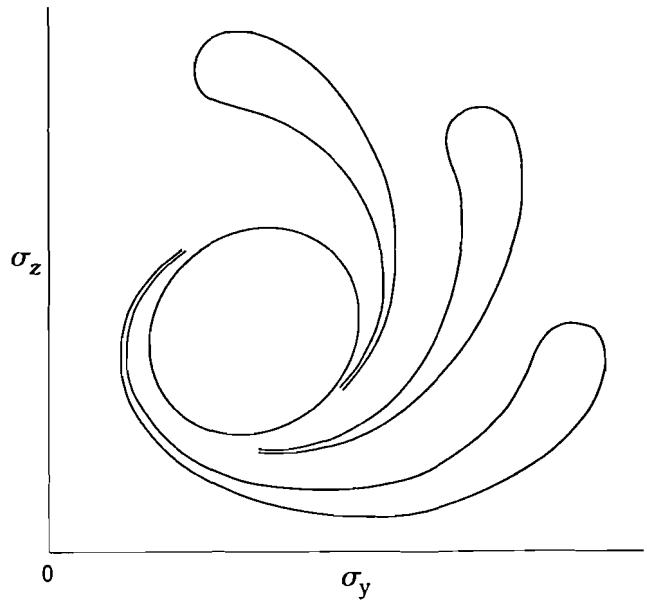

Figure 13. A qualitative sketch of the flip bifurcation curves (see Figure 8) spiraling around the internal boundary of the annular chaotic region.

6. Summary and Conclusions

The very high (actually infinite) number of equilibria and cycles involved by the bifurcation curves of model (1-5) is a serious obstacle for a clear biological interpretation of the dynamic behavior of the food chain. Nevertheless, if the final target of the analysis is the classification of the stable modes of behavior of the system, all saddle equilibria and saddle cycles must be disregarded, because the attention must only be focused on the attractors. Moreover, if the attractors present in the very narrow band surrounding the chaotic region are also disregarded, only five of them remain. They are the following

E, a tri-trophic equilibrium

$\hat{C}$, a tri-trophic cycle with quite low predator densities and high frequency and high amplitude prey oscillations (see Figure 6a)

C, a tri-trophic cycle characterized by high predator densities and relatively low prey densities (see Figure 6b)

A, a tri-trophic strange attractor [in general a "tea-cup" strange attractor (see Figure 2)]

$\tilde{C}$, a di-trophic cycle characterized by the absence of the predator population.

The first attractor corresponds to stationary coexistence, the second and third to cyclic coexistence, the fourth to chaotic coexistence, while the fifth corresponds to extinction of the

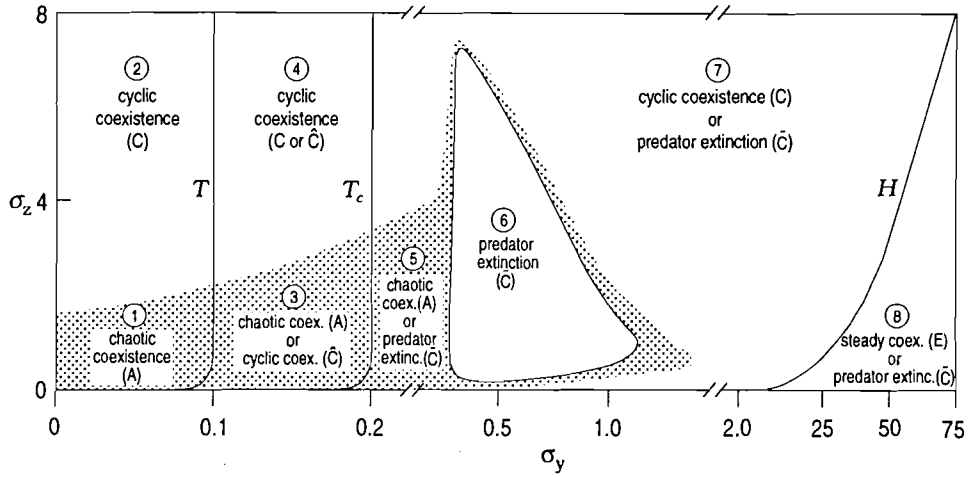

Figure 14. The partition of the parameter space into eight regions of different asymptotic behavior (see Figures 3, 5, and 7).

top population of the food chain. For suitable combinations of prey and predator body sizes there is only one attractor, but for others there are two alternative attractors.

Figure 14 (based on Figures 3, 5, and 7) summarizes all possibilities by partitioning the parameter space in eight regions. In region 1, containing the origin, there is only one attractor, namely the tea-cup strange attractor A. This is so because the reference parameter setting gives rise to a reduced model (6-8) [obtained from (1-5) for body sizes tending to zero] which is chaotic. In region 2 the attractor (still unique) is the cycle C obtained from A through a reverse cascade of flip and tangent bifurcations. Thus, in regions 1 and 2 coexistence (either chaotic or cyclic) is the only possible mode of behavior. This is true also in regions 3 and 4 where, nevertheless, there are two alternative regimes of coexistence: one chaotic (A) and one cyclic ($\hat{C}$) in region 3 and two cyclic (C and $\hat{C}$) in region 4. In regions 5, 7, and 8 both coexistence [chaotic (A), cyclic (C) or stationary (E)] and predator extinction ($\tilde{C}$) are possible, while in region 5 extinction of the top population is the only possible mode of behavior.

Figure 14 can be used to interpret the role played by dispersal in metapopulation systems (see Taylor, 1990). Moving away from the origin of Figure 14, i.e., increasing continuously the body sizes of prey and predator individuals, one goes through regions characterized by more and more regular attractors. For example, moving along the σ_z axis the strange attractor A becomes a cycle C, while moving along the σ_y axis the strange attractor A is first transformed into a cycle (C) and then into an equilibrium (E). This is in agreement with a conjecture made by Hastings (1993) on the stabilizing influence of dispersal, bringing to the conclusion that "chaotic dynamics may be less prevalent than the study of models without spatial structure would indicate".

Region 6 is of particular importance for interpreting the difficulties often encountered in practice in trying to control a pest biologically. Indeed, if the prey is a pest feeding on a plant

of commercial value, one can consider the possibility of introducing a predator in order to keep the prey in check. But Figure 14 shows that when the body size σ_y of the pest is in the range corresponding to region 6, only predators with extreme body sizes (either very small or very large) can keep the pest under control, while all predators with more reasonable body sizes cannot perform this task.

It is also interesting to remark that the bifurcation structure of model (1-5) recalls that of the Rosenzweig–McArthur food chain model (6-8). Indeed, the complex cascade of intersecting flip and tangent bifurcation curves which gives rise to the outside boundary of the chaotic region (see Figure 8) is present also in model (6-8) (Klebanoff and Hastings, 1994; McCann and Yodsiz, 1995a; Kuznetsov and Rinaldi, 1995). Also the crisis of the strange attractor A, determining the boundary of the region of unavoidable predator extinction (region 6 of Figure 14), has been notice by McCann and Yodsiz (1995b) for the Rosenzweig–McArthur food chain.

Finally, it is important to stress, once more, that the results summarized by Figure 14 are valid only for the particular parameter setting selected for the analysis. Unfortunately, a paramount effort would be required to establish, through numerical analysis, if these results are robust. A more reasonable task along this line would be that of repeating the analysis carried out in this paper for parameter settings interpreting biological communities of particular relevance.

Acknowledgment

The authors would like to thank V.A.A. Jansen for stimulating discussions on the problem.

References

Abrams, P., Roth, J.: The effects of enrichment of three-species food chains with nonlinear responses. Ecology, **75**, 1118–1130 (1994a)

Abrams, P., Roth, J.: The responses of unstable food chains to enrichment. Evol. Ecol., **8**, 150–171 (1994b)

Arnold, V.I.: Geometrical Methods in the Theory of Ordinary Differential Equations. Berlin Heidelberg New York: Springer-Verlag 1983

Diekmann, O., Metz, J.A., Sabelis, M.W.: Mathematical models of predator/prey/plant interactions in a patch environment. Exp. Appl. Acarol., **5**, 319–342 (1988)

Grebogi, C., Ott, E., Yorke, J.A.: Crises, sudden changes in chaotic attractors, and transient chaos. Physica D, **7**, 181–200 (1983)

Guckenheimer, J., Holmes, Ph.: Nonlinear Oscillations, Dynamical Systems and Bifurcations of Vector Fields. Berlin Heidelberg New York: Springer-Verlag 1983

Hastings, A.: Complex interactions between dispersal and dynamics: Lessons from coupled logistic equations. Ecology, **74**, 1362–1372 (1993)

Hastings, A., Powell, T.: Chaos in a three species food chain. Ecology, **72**, 896–903 (1991)

Jansen, V.A.A.: Effects of dispersal in a tri-trophic metapopulation model. J. Math. Biol. (1995) in press

Jansen, V.A.A., Sabelis, M.W.: Prey dispersal and predator persistence. Exp. Appl. Acarol., **14**, 215–231 (1992)

Khibnik, A.I., Kuznetsov, Yu.A., Levitin, V.V., Nikolaev, E.V.: Continuation techniques and interactive software for bifurcation analysis of ODEs and iterated maps, Physica D, **62**, 360–370 (1993)

Klebanoff, A., Hastings, A.: Chaos in three species food chains. J. Math. Biol., **32**, 427–451 (1994)

Kuznetsov, Yu.A., Rinaldi, S.: Remarks on food chain dynamics. Centrum voor Wiskunde en Informatica, Amsterdam, The Netherlands, CWI Report AM-R9513 (1995) to appear in Math. Biosc.

Kuznetsov, Yu.A., Muratori, S., Rinaldi, S.: Homoclinic bifurcations in slow-fast second order systems, Nonlinear Anal., **22**, (1995)

Levins, R.: Some demographic and genetic consequences of environmental heterogeneity for biological control. Bull. Entomol. Soc. Amer., **15**, 237–240 (1969)

Levins, R.: Extinction. Lectures on Mathematics in Life Sciences, **2**, 77–107 (1970)

McCann, K., Yodsiz, P.: Biological conditions for chaos in a three species food chain. Ecology, **75**, 561–564 (1994)

McCann, K., Yodsiz, P.: Bifurcation structure of a three species food chain model. Theor. Pop. Biol., **48** (1995a)

McCann, K., Yodsiz, P.: Nonlinear dynamics and population disappearances. The Amer. Natur. (1995b)

Muratori, S.: An application of the separation principle for detecting slow-fast limit cycles in a three-dimensional system. Appl. Math. Comp., **43**, 1–18 (1991)

Muratori, S., Rinaldi, S.: A separation condition for the existence of limit cycles in slow-fast systems. Appl. Math. Model, **15**, 312–318 (1991)

Muratori, S., Rinaldi, S.: Low- and high-frequency oscillations in three-dimensional food chain systems. SIAM J. Appl. Math., **52**, 1688–1706 (1992)

Rinaldi, S., Muratori, S.: Slow-fast limit cycles in predator-prey models. Ecol. Model, **61**, 282–308 (1992)

Sabelis, M.W., Diekmann, O., Jansen, V.A.A.: Metapopulation persistence despite local extinction: Predator-prey patch models of the Lotka-Volterra type. Biol. J. Linn. Soc., **42**, 267–283 (1991)

Scheffer, M.: Should we expect strange attractors behind plankton dynamics and if so, should we bother? J. Plankton Res., **13**, 1291–1305 (1991)

Taylor, A.D.: Metapopulations, dispersal, and predator-prey dynamics: An overview. Ecology, **71**, 429–434 (1990)